

Therefore, we need to introduce something a new technique for the Fourier transformation of general resistive circuits driven by the periodic input. The circuit model is shown in Fig.1, where each Fourier coefficient for the function $i = f(v)$ can be numerically calculated in the following formula:

$$\left. \begin{aligned} I_0 &= \frac{1}{2\pi} \int_0^{2\pi} f(v) dt \\ I_{2k-1} &= \frac{1}{\pi} \int_0^{2\pi} f(v) \cos k\omega t dt, \quad I_{2k} = \frac{1}{\pi} \int_0^{2\pi} f(v) \sin k\omega t dt \\ k &= 1, 2, \dots, M \end{aligned} \right\} \quad (3)$$

Let us apply the trapezoidal integration formula to (3) as follows;

$$\int_a^b f(v) dt = \frac{h}{2}(f_0 + f_n) + h(f_1 + f_2 + \dots + f_{n-1}) \quad (4)$$

where the step-size of the integration is $h = (a-b)/n$. Then, the truncation error is given by $f^{(2)}h^2/12n$. Using this formula, we will realize the equivalent circuit model satisfying (3) with ABMs of Spice. To understand the circuit model, we assume that the input is

$$v(t) = V_0 + \sum_{k=1}^M (V_{2k-1} \cos k\omega t + V_{2k} \sin k\omega t) \quad (5)$$

We set $\theta = \omega t$. The **Fourier transfer circuit model** for calculating the N th higher harmonic components is shown by Fig.1. A number of $2K + 1$ blocks calculate the N th components using (3) which is composed of the nonlinear resistive circuits and ABMs of Spice. On the other hand, the integration interval $[0, 2\pi]$ is divided by $2K$ sections using $2K$ resistors, so that each input node voltage of the ABM blocks is given by $\theta_k = 2\pi k/2K$ at the k th node. Thus, the resultant current sources are given by $f(\mathbf{V}, \theta_k) \cos N\theta_k, f(\mathbf{V}, \theta_k) \sin N\theta_k, k = 1, 2, \dots, 2K$. Summing them, their outputs correspond to the coefficients of $\cos N\theta$ and $\sin N\theta$.

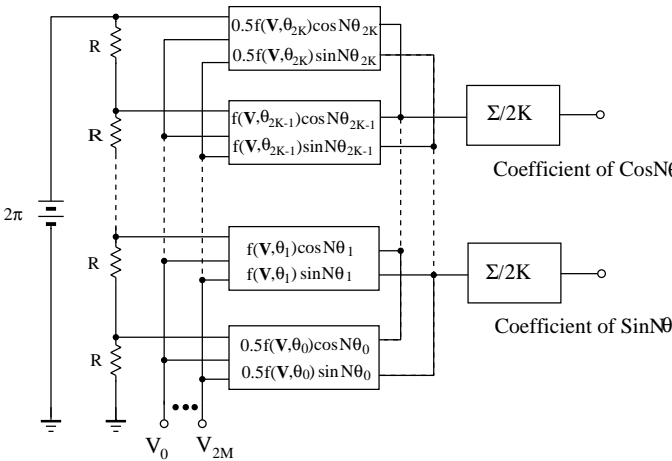


Fig.1 Fourier transfer circuit model.

The fact that the circuit model is only composed of the resistive circuits is important for the calculation of the frequency response curves with the curve tracing algorithm [12].

To investigate the numerical accuracy, we first calculate a **modified Bessel function** as follows;

$$I_N(x) = \frac{1}{2\pi} \int_{-\pi}^{\pi} e^{x \cos \theta} \cos N\theta d\theta \quad (6)$$

The simulation results with $h = 2\pi/20$ is shown in Fig.2. The value $I_1(10) = 2761$ at $N = 1, x = 10$ is exactly equal to the result from the Table of Bessel function [10]. Note that this kind of Fourier expansion for the exponential function is very important to the analysis of the circuit containing diodes and bipolar transistors [5].

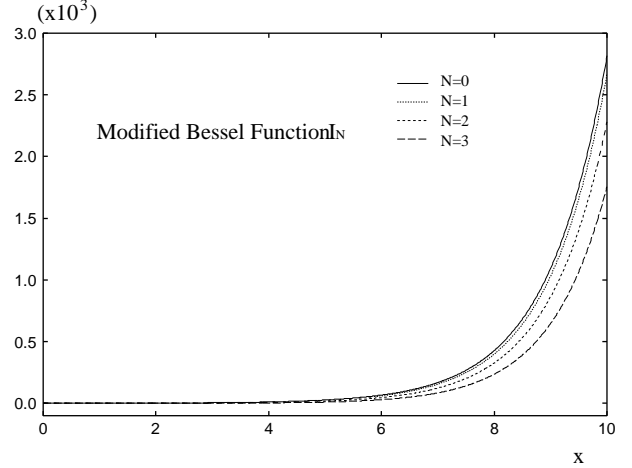


Fig.2 Fourier transformation for modified Bessel function.

Next, we apply it to the Fourier expansion of **MOSFET**, whose characteristic in the Spice model is described by a piecewise continuous function [5] as follows:

1. Linear region: ($V_{GS} > V_T, V_{GS} - V_T \geq V_{DS} > 0$)

$$I_D = \frac{KW}{L} \left[(V_{GS} - V_T) - \frac{V_{DS}}{2} \right] V_{DS} (1 + \lambda V_{DS}) \quad (7.1)$$

2. Saturation region: ($V_{GS} > V_T, V_{DS} > V_{GS} - V_T$)

$$I_D = \frac{KW}{L} (V_{GS} - V_T)^2 (1 + \lambda V_{DS}) \quad (7.2)$$

The result of Fourier expansions for the input $V_{GS} \cos \omega t$ is shown in Fig.3.

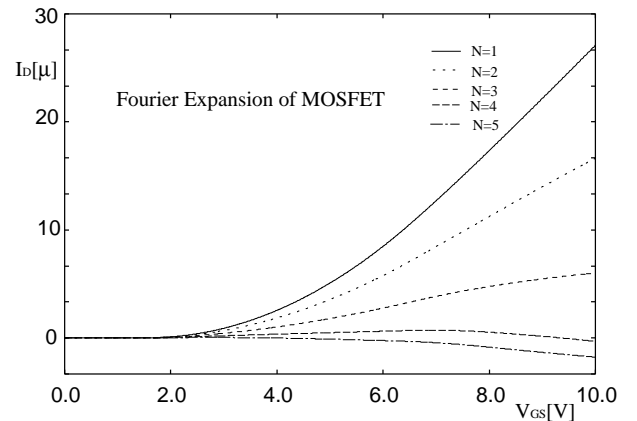


Fig.3 Fourier transformation for MOSFET.
 $V_{DS} = 3[V], K = 3.87[\mu A], \lambda = 0.01605,$
 $W = 2[\mu m], L = 2[\mu], V_T = 0.827[V]$

Thus, the Fourier transfer circuit model shown in Fig.1 can be efficiently applied to any kind of circuit elements contained in analog integrated circuits.

3. Frequency response curves of nonlinear circuits

Nowadays, the frequency response curves of the fundamental frequency (H_1), the second harmonic distortion (HD_2), the third harmonic distortion (HD_3) and so on are usually calculated by the use of the Volterra series method [3], where the nonlinear characteristics must be described by the power series functions. On the other hand, our distortion analysis using the Fourier transfer circuit model can be efficiently applied to the circuits containing any type of the elements described by exponential, piecewise linear functions and others. To understand our harmonic balance method, we consider the following circuit equation;

$$\mathbf{f}(\dot{\mathbf{v}}, \mathbf{v}, \mathbf{w}, \omega t) = \mathbf{0}, \quad \mathbf{f} : R^{2n+m} \mapsto R^{n+m} \quad (8)$$

Although the steady-state waveforms may contain many higher harmonic components, for simplicity, we consider only the DC and fundamental frequency components as follows;

$$\left. \begin{aligned} \mathbf{v}(t) &= \mathbf{V}_0 + \mathbf{V}_1 \cos \omega t + \mathbf{V}_2 \sin \omega t \\ \mathbf{w}(t) &= \mathbf{W}_0 + \mathbf{W}_1 \cos \omega t + \mathbf{W}_2 \sin \omega t \end{aligned} \right\} \quad (9)$$

Substituting (9) into (8) and applying the harmonic balance method, we have the following **determining equation**;

$$\left. \begin{aligned} \mathbf{F}_0(\mathbf{V}_0, \mathbf{V}_1, \mathbf{V}_2, \mathbf{W}_0, \mathbf{W}_1, \mathbf{W}_2, \omega) &= \mathbf{0} \cdots \text{DC} \\ \mathbf{F}_c(\mathbf{V}_0, \mathbf{V}_1, \mathbf{V}_2, \mathbf{W}_0, \mathbf{W}_1, \mathbf{W}_2, \omega) &= \mathbf{0} \cdots \cos \omega t \\ \mathbf{F}_s(\mathbf{V}_0, \mathbf{V}_1, \mathbf{V}_2, \mathbf{W}_0, \mathbf{W}_1, \mathbf{W}_2, \omega) &= \mathbf{0} \cdots \sin \omega t \end{aligned} \right\} \quad (10)$$

In generally, although the equation (10) can be obtained by the application of the harmonic balance method to the circuit equation, it is really troublesome task. We propose a Spice-oriented algorithm for getting the relations (10) from the DC-circuit, Cosine-circuit and Sine-circuit, directly.

- a. **Inductive elements**: Assume that the nonlinear inductor is described by current-controlled characteristic as follows;

$$\phi_L = \hat{\phi}_L(i_L) \quad (11.1)$$

For the inductor current,

$$i_L = I_{0,L} + \sum_{k=1}^M (I_{2k-1,L} \cos k\omega t + I_{2k,L} \sin k\omega t), \quad (11.2)$$

we have

$$\left. \begin{aligned} v_L(t) &= \frac{\partial \hat{\phi}_L}{\partial i_L} \frac{di_L}{dt} \\ &= \left(\Phi_{0,L} + \sum_{k=1}^M (\Phi_{2k-1,L} \cos k\omega t + \Phi_{2k,L} \sin k\omega t) \right) \\ &\times \left(\sum_{k=1}^M k\omega (-I_{2k-1,L} \sin k\omega t + I_{2k,L} \sin k\omega t) \right) \\ &\simeq V_{0,L} + \sum_{k=1}^M (V_{2k-1,L} \cos k\omega t + V_{2k,L} \sin k\omega t) \end{aligned} \right\} \quad (11.3)$$

where $\Phi_{0,L}$, $\Phi_{2k-1,L}$ and $\Phi_{2k,L}$ are function of $\{I_{0,L}, I_{2k-1,L}, I_{2k,L}\}$. They are calculated by the Fourier transfer circuit shown by Fig.1.

For the linear inductor L , the coefficient are simply given by the linear current-controlled voltage sources $k\omega LI_{2k,L}$ in the Cosine-circuit and $-k\omega LI_{2k-1,L}$ in the Sine-circuit, respectively [9].

- b. **Capacitive elements**: High frequency bipolar transistor and MOFET models [5] usually contain nonlinear depletion and diffusion capacitors which are described by the voltage-controlled characteristics as follow;

$$q_C = \hat{q}_C(v_C) \quad (12.1)$$

For the capacitor voltage,

$$v_C = V_{0,C} + \sum_{k=1}^M (V_{2k-1,C} \cos k\omega t + V_{2k,C} \sin k\omega t), \quad (12.2)$$

we have

$$\left. \begin{aligned} i_C(t) &= \frac{\partial \hat{q}_C}{\partial v_C} \frac{dv_C}{dt} \\ &= \left(Q_{0,C} + \sum_{k=1}^M (Q_{2k-1,C} \cos k\omega t + Q_{2k,C} \sin k\omega t) \right) \\ &\times \left(\sum_{k=1}^M k\omega (-V_{2k-1,C} \sin k\omega t + V_{2k,C} \sin k\omega t) \right) \\ &\simeq I_{0,C} + \sum_{k=1}^M (I_{2k-1,C} \cos k\omega t + I_{2k,C} \sin k\omega t) \end{aligned} \right\} \quad (12.3)$$

where $Q_{0,C}$, $Q_{2k-1,C}$ and $Q_{2k,C}$ are function of $\{V_{0,C}, V_{2k-1,C}, V_{2k,C}\}$, and they are also estimated by the Fourier transfer circuit shown in Fig.1.

For the linear capacitor C , the Fourier coefficients are given by the linear voltage-controlled current sources $k\omega CV_{2k,C}$ in the Cosine-circuit and $-k\omega CV_{2k-1,C}$ in the Sine-circuit, respectively [9].

Note that the inductive elements in the DC-circuit are removed by the shorted-circuits, and the capacitive elements by the opened-circuits.

Thus, all the circuit topologies corresponding to the DC, Cosine-circuits and Sine-circuits for the higher harmonic components are equal to the original circuit, but they are coupled in each other with the controlled sources.

4. An illustrative example

Now, consider distortion analysis of a simple high frequency amplifier [3] shown by Fig.4(a). The Ebers-Moll model of transistor [5] is shown by Fig.4(b), where the diode models are given by

$$\begin{aligned} i_{D1} &= 10^{-14} \{ \exp(40v_{be} - 1) \} [A], \\ i_{D2} &= 10^{-14} \{ \exp(40v_{bc} - 1) \} [A] \end{aligned}$$

and

$$\begin{aligned} R_s &= 10[k\Omega], \quad R_L = 10[k\Omega], \quad V_s = 800[mV] \\ \alpha_F &= 0.99, \quad \alpha_R = 0.3 \end{aligned}$$

$$C_1 = 10+10v_{bc}^3[pC], \quad C_2 = 10+10v_{be}^3[pC], \quad v_{in} = V_{m,in} \cos \omega t$$

For calculating the frequency response of the fundamental, the second order distortion (HD_2) and the third order distortion (HD_3), we assumed the waveforms as follows;

$$\begin{aligned} v_{be} &= V_{be,0} + \sum_{k=1}^3 (V_{be,2k-1} \cos k\omega t + V_{be,2k} \sin k\omega t) \\ v_{bc} &= V_{bc,0} + \sum_{k=1}^3 (V_{bc,2k-1} \cos k\omega t + V_{bc,2k} \sin k\omega t) \end{aligned}$$

Applying the harmonic balance method, we obtained the DC, Cosine-circuit and Sine-circuit as shown in Fig.4 (c), (d) and (e), respectively. The circuit models for calculating the higher order distortions can be obtained in the same manner. Note that I_{C0} , I_{E0} in the figure are the DC i voltage-controlled current sources, and $(I_{C,k}, I_{E,k}, k = 1, 2, 3)$ are given by the functions of the input frequency ω . These controlled sources can be calculated by the use of Fourier transfer circuit model shown in Fig.1.

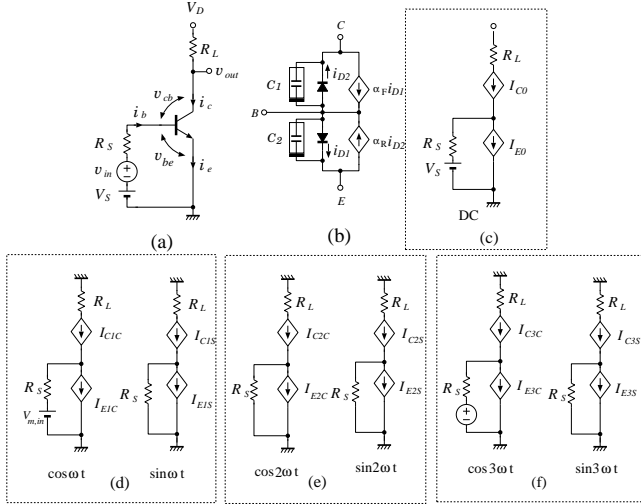


Fig.4 (a) Amplifier circuit, (b) High frequency Ebers-Moll model, (c) DC-circuit, (d) Cosine-circuit, (e) Sine-circuit

Continuously changing the input frequency ω , we can obtain the frequency response curves for the distortion analyses for the fundamental, HD₂ and HD₃ as shown in Fig.5, which is almost the same as those of reference [3].

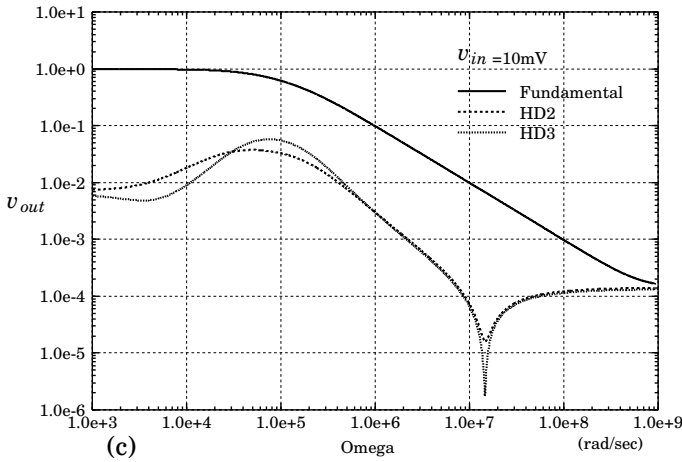


Fig.5 Distortion analysis.

5. Conclusions and remarks

The frequency domain distortion analysis is very important for designing the high frequency analog integrated circuits. It has been usually carried out by the Volterra series method, where the nonlinear characteristics should be described by the power series function in the vicinity of the DC operating point. Thus, the method can be only applied

to the weakly nonlinear circuits. Furthermore, the higher order kernels of the Volterra series are complicate, so that it is usually restricted to the analysis of relatively low order distortion analysis [3].

In this paper, we proposed an efficient Spice-oriented distortion analysis based on the harmonic balance method, where we proposed the Fourier transfer circuit model. The model can be efficiently applied to any kind of nonlinear elements described by such as exponential and piecewise continuous functions and/or resistive circuits. We also proposed the DC, Cosine and Sine circuits corresponding to the determining equation of the harmonic balance method, whose circuit topologies are equal to the original circuit. Thus, the algorithm of our distortion analysis is quite simple and user-friendly. We are going to apply the algorithm to the complicated circuits such as the modulators.

REFERENCES

- [1] M.Schetzen, *The Volterra and Wiener Theorems of Nonlinear Systems*, John Wiley and Sons, 1978.
- [2] D.D.Weiner and J.E.Spina, *Sinusoidal Analysis and Modeling of Weakly Nonlinear Circuits with Application to Nonlinear Interference Effects*, Van Nostrand Reinhold, 1980.
- [3] P.Wambacq and W.Sansen, *Distortion Analysis of Analog Integrated Circuits*, Kluwer Academic Pub., 1998.
- [4] L.O.Chua and C-Y.Ng, "Frequency-domain analysis of nonlinear systems: formulation of transfer functions," *IEE Trans. Electronic Circuits and Systems*, Vol.3, no.6, pp.257-269, 1979.
- [5] R.L.Geiger, P.E.Allen and N.R.Strader, *VLSI: Design Techniques for Analog and Digital Circuits*, McGraw-Hill, 1990.
- [6] T.J.Aprille and T.N.Trick, "Steady-state analysis of nonlinear circuits with periodic input," *Proc. IEEE*, vol.60, pp.108-114, 1972.
- [7] K.S.Kundert, J.K.White and A.Sangiovanni-Vincentelli, *Steady-State Methods for Simulating Analog and Microwave Circuits*, Kluwer Academic Pub., 1990.
- [8] A.Ushida, T.Adachi and L.O.Chua, "Steady-state analysis of Nonlinear Circuits based on hybrid methods," *IEEE Trans. on Circuits and Systems-I: Fundamental Theory and Applications*, vol.39, no.9, pp.649-661, 1992.
- [9] A.Ushida, Y.Yamagami and Y.Nishio, "Frequency responses of nonlinear networks using curve tracing algorithm," *ISCAS 2002*, vol.I, pp.641-644, 2002.
- [10] K.K.Clarke and D.T.Hess, *Communication Circuits: Analysis and Design*, Addison-Wesley Pub. Co., 1971.
- [11] S.Wolfram, *Mathematica*, Addison-Wesley Pub. Co., 1988.
- [12] A.Ushida, Y.Yamagami, Y.Nishio, I.Kinouchi and Y.Inoue, "An efficient algorithm for finding multiple DC solutions based on the SPICE-oriented Newton homotopy method," *IEEE Trans. on CAD*, vol.21, no.3, pp.337-348, 2002.